Journal of Thermal Analysis and Calorimetry (2021) 146:1121–1131
https://doi.org/10.1007/s10973-020-10099-x

Thermal techniques as a tool for the direction of the preparation of photocatalytically efficient titania thin films and powders

Petra Horvat[1,2] · Andrijana Sever Škapin[2] · Urška Lavrenčič Štangar[1] · Romana Cerc Korošec[1]

Received: 26 February 2020 / Accepted: 17 July 2020 / Published online: 3 August 2020

Abstract
Photocatalytically active titania thin films and powders were prepared via sol–gel route from $TiCl_4$ precursor. Organic polymer hydroxypropyl cellulose was added into sol in order to increase active surface area. Thin films were deposited onto substrates using dip-coating technique. Thin films and xerogels were thermally treated in a muffle furnace to a different extent. Temperature of heat treatment was determined using thermogravimetry and differential scanning calorimetry, while X-ray diffraction was used to identify the formation of the anatase phase, eventual presence of other crystalline formations and the average particle size. The shape and size of the pores of the selected thin films were analyzed using SEM, while specific surface area of selected thermally treated xerogels was determined using Brunauer–Emmett–Teller (BET) surface area analysis. Measurements of photocatalytic efficiency of thin films and powders were performed by FT-IR spectroscopy; for thin films on the basis of diminishing C–H stretching vibrations of model fatty compound methyl stearate during irradiation with UVA light, while in the case of powders the oxidation of isopropanol into acetone was the model photocatalytic reaction. Obtained results confirm that different factors, such as particle size, porosity, thickness of thin film, the presence and type of crystalline titania modification have a substantial effect on photocatalytic efficiency of prepared titania materials.

Keywords Titania · Thin films · Xerogels · Photocatalysis · Thermogravimetry · DSC

Introduction

Owing to its exceptional physico-chemical properties, i.e., chemical stability, inertness, white colour, high refractive index and non-toxicity in the micro-size level, TiO_2 is the most widely used white pigment [1]. Photoinduced processes, originated from its semiconductor properties, become prominent with increasing specific surface area, which is achieved by decreasing titania particle size. In this perspective and due to its high activity, stability and low cost, TiO_2 have been extensively used as a material for environmental remediation purposes and for energy conversion and remain the most widely used semiconductor for photocatalytic applications [2–8].

Active species, such as superoxide and hydroxyl radical, are formed when UV light with the energy equal or higher than that of the band gap irradiates the surface of TiO_2 particle (in the case of anatase wavelength should be lower than 380 nm). Both radicals are very reactive and initiate redox reaction with adsorbed organics, causing their degradation into mineral substances, mostly CO_2 and H_2O. Parallel to above-mentioned reactions, photoinduced hydrophilic conversion of the TiO_2 surface also takes place [9]. For the photocatalytic experiments, TiO_2 is mostly used in a powder form [10]. In the case that heterogeneous photocatalysis occurs in a solid–liquid system, the major drawback is the particle–fluid separation for the catalyst recycling. This trouble can be avoided using immobilized titania thin film on a support. Besides, harmful release of nanoparticles to environment is also prevented. However, there are certain drawbacks regarding the immobilization of TiO_2, especially lower photocatalytic efficiency due to the decreased catalyst surface in immobilized TiO_2 [11].

Sol–gel method enables preparation of thin films as well as corresponding xerogels. A translucent sol is formed after hydrolysis of the TiO_2 precursor, which can be coated on the

✉ Romana Cerc Korošec
romana.cerc-korosec@fkkt.uni-lj.si

[1] Faculty of Chemistry and Chemical Technology, University of Ljubljana, Večna pot 113, 1000 Ljubljana, Slovenia

[2] Slovenian National Building and Civil Engineering Institute, Dimičeva 12, 1000 Ljubljana, Slovenia

substrates and thermally treated at higher temperatures to promote crystallization of photocatalytically active material. On the other hand, photocatalytically efficient crystalline titania powder can be prepared by thermal treatment of the amorphous photocatalitically non-active xerogel, obtained by drying the prepared sol. Alkoxide sol–gel route enables easy preparation procedure, but high cost of the precursors and strict control of the synthesis conditions limited the commercialization on larger scale. If inorganic salts are used as precursors, the acidic nature of TiO_2 sol limits the choice of substrates [12]. Environmental interest for waste-water and air treatment is oriented to development and optimization of an inexpensive and technologically simple route for the preparation of self-cleaning and superhydrophilic titania thin films and powders, suitable for industrial production. Some of the demands for such production can be met by the particulate sol–gel method, where $TiCl_4$ is selected as a precursor.

A degree of thermal treatment is very important step in the preparation of photocatalytically efficient thin film or powders. Not only the crystalline phase, but also the size of the grains, crystallization degree and agglomeration of particles determine the properties of the final material [13]. For preventing agglomeration and increasing surface area, different organic polymers can be added to the sol. During thermal treatment, their combustion leads to formation of pores in the structure [14].

Two opposite effects influence the photocatalytic activity as particle diameter size of titania decreases: active surface area for catalytic reaction is higher and in the semiconducting material recombination rate of photo-induced electron–hole pairs decreases due to faster arrival to the reaction sites on the surface [15]. However, results of different studies have shown that the photocatalytic activity does not monotonically increase with decreasing particle size. This was attributed to higher recombination rate in samples with particle sizes, smaller than 6 nm [16]. On the other hand, bandgap becomes wider with decrease in the particle size, meaning that shorter wavelength is needed for excitation [17]. Additionally, the amorphous fraction of TiO_2 can also have a detrimental effect on photocatalytic activity [18], while decreased photocatalytic efficiency is caused by grain growth due to calcination at higher temperatures [19]. At elevated temperatures anatase crystalline phase begins to transform to the most thermodynamically stable phase, rutile, which has a little narrower bandgap with regard to anatase (3.0 eV vs 3.2 eV) [20]. Lower number of hydroxyl groups on the surface of rutile and also its lower oxidation potential compared to anatase leads to decrease in its photocatalytic performance [21]. Anatase modification of titania is therefore considered as the most photocatalytically efficient [22] and due to the factors, which influence the activity, it is reasonable to find an optimal crystallite size.

The aim of the work was to monitor the crystallization process during thermal treatment of sol–gel prepared thin films and corresponding xerogels using thermogravimetry, differential scanning calorimetry and XRD. The size of the nano-crystallites was calculated from XRD patterns using the Scherrer equation, while photocatalytic efficiency of thin films and powders, thermally treated to a different degree, was determined using two different methods. Within this work, we demonstrated that with systematic approach and modification of different parameters, such as temperature and time of thermal treatment, and addition of organic polymer, efficient photocatalytically active titania films and powders can be successfully prepared.

Experimental

Sol–gel synthesis and preparation of thin films and powders

Sols were synthesized according to the following procedure: cooled deionized water was acidified with 12 M H_2SO_4 solution. Inorganic precursor $TiCl_4$ (Merck) with 10% excess with regard to stoichiometric volume was added dropwise into cold deionized water at 12 °C to obtain approximately 0.5 M concentration of Ti^{4+} ions. Temperature increased to 37 °C and pH decreased to 1.0. Solution was gently stirred with a magnetic stirrer for additional 48 h to obtain transparent sol which was stable for more than 6 months. 0.3 mass% of organic polymer hydroxypropyl cellulose (HPC, $M_w = 105$ g/mol, S-Aldrich) with regard to the mass of the sol was added to the sol to increase the viscosity of the sol and also the porosity after thermal treatment.

Thin films were prepared using a dip-coating technique. Silicon resins, microscope-cover glasses and platinum foils were used as a substrate. All used substrates are thermally inert under temperature range used for the preparation of thin films. The thickness of the thin film was modified by changing the withdrawal speed; thicker thin films were obtained using higher speeds. After deposition, substrates with deposited films were left to dry; solvent evaporated and the thin layer condensed into a gel. Thermal treatment was performed in a muffle furnace at different temperatures, i.e., 470 °C, 500 °C, 550 °C, 600 °C and 700 °C. Duration of thermal treatment was from 15 to 60 min.

TiO_2 powders were prepared by thermal treatment of xerogels, which were obtained by drying a certain volume of the prepared sols. Temperature of thermal treatment was 630 °C, 700 °C and 750 °C; and duration was 30 min.

Characterization

TGA analyses were performed on a Mettler Toledo TGA/SDTA 851^e Instrument in a temperature range from 25 to 750 °C. Heating rate was 5 K min^{-1}. 150 µL platinum crucibles were used. During the measurements, the furnace was purged with air (100 mL min^{-1}). Baseline was subtracted. Thin films were deposited onto microscope-cover glasses and after drying cut into small pieces, suitable for placing into a crucible. Xerogels with the initial mass of around 5 mg were analyzed with the same temperature protocol. In the case of TG-MS measurements, evolved gasses were analyzed with a Pfeiffer Vacuum ThermoStar mass spectrometer, coupled to TGA/DSC1 instrument. Gasses were introduced into mass spectrometer via 75-cm long heated capillary.

DSC analyses were performed on a Mettler Toledo DSC 822^e. Thin films were coated onto the platinum foil (0.7 cm × 0.7 cm), dried and placed directly onto the thermocouple. Bare platinum foil served as a reference. Xerogels were weighed into 70 µL platinum pan; in this case, empty pan served as a reference. The same measurement conditions as for TG measurements were used except the upper temperature, which was 700 °C.

FE-SEM analyses were performed using a Carl Zeiss, Supra 35 VP field emission scanning electron microscope (FE-SEM). FE-SEM was used to measure the thickness of the thin film, morphology and to observe the porosity.

The qualitative and semi-quantitative elemental analyses of thermally treated xerogels were performed by energy-dispersive X-ray spectroscope (EDX, Oxford Instruments, Great Britain) using the INCA software. The accelerating voltage of 18 kV was used. Quantitative analyses were done considering all elements analyses.

The BET surface area was measured by a surface area analyzer via nitrogen adsorption–desorption isotherms at liquid nitrogen temperature using a Micrometrics ASAP 2020 instrument.

XRD patterns were recorded using X-ray diffractometer PANalytical X'Pert PRO (CuKα_1 irradiation 1.5406 Å) between 24 and 32 2 Θ with 0.034° per second and integration time of 500 s. Silicon resins with the size 22 × 22 mm^2 were used as substrates. Crystallite size was calculated using Scherrer formula from the broadening of the reflection at 25.4° 2Θ.

Photocatalytic efficiency of the prepared films was determined on the basis of a model pollutant methyl stearate (MS) degradation, influenced by UV irradiation. For this purpose, thin films were deposited on a silicon substrate. After thermal treatment of titania thin films, model pollutant was introduced on the surface. 0.1 M solution of methyl stearate in 1-octanol was prepared and deposited by dip-coating technique. Degradation of MS during UV irradiation was monitored with FT-IR spectroscopy (Perkin Elmer Spectrum 100 spectrophotometer). Diminishing of peak heights, originating from C-H stretching modes, was monitored with increasing illumination time. UV irradiation chamber consisted of 3 light sources with maximum intensity at 320 nm and irradiation density 2 mW/cm^2.

Photocatalytic activity of powders was determined monitoring the oxidation of iso-propanol into acetone in a homemade sealed reactor system. The system consists of a cylindrical reactor, gas chamber, FT-IR spectrometer (Perkin Elmer Spectrum BX with Timebase software), 300 W xenon light source (Newport Oriel Instrument, USA), membrane pump, PFTE tubes and molecular sieves. Method, described in detail elsewhere [23–25] was used. In the continuation, the samples preparation and measuring procedure are briefly described.

Selected volume of sol was poured into an ashing crucible and left to dry. Xerogels were thermally treated for 30 min at temperatures, based on the results of TG and DSC analyses. Obtained powders were grinded in an agate mortar. 50 mg of fine powders were dispersed in butanol and poured into a petri dish with 50 mm diameter. After the solvent evaporated, samples were dried in a laboratory dryer at 80 °C for additional 10 min. As a reference, we have prepared P25 (Evonik) in the same way.

Individual sample was placed in a cylindrical reactor chamber and hermetically closed using quartz glass. Working distance between sample and light source was approximately 4 cm, while mean UV light intensity was 2 mW cm^{-2}. Air in the chamber was dried using molecular sieves to obtain 25 ± 5% relative humidity. All measurements were carried out at 23 ± 3 °C. When we obtained desired conditions gas flow, 3 µL of iso-propanol (approx. 700 ppm in gaseous phase) was injected into the cell. Its concentration was being decreased due to adsorption onto the sample and the walls of the reaction chamber. When the concentration of iso-propanol slowly stabilized, UV light was turned on. Iso-propanol concentration decreased and at the same time acetone concentration started increasing. Initial slope of the formation of acetone presented the photocatalytic activity of powders. Absorbance bands for both iso-propanol (951 cm^{-1}) and acetone (1207 cm^{-1}) were monitored for several hours. The activity of blank sample is zero what we have proved in previous work [24].

Results and discussion

Thermal analysis

A comparison of TG-MS curves of the primary xerogel (prepared without addition of HPC), and xerogel prepared with addition of HPC, is presented in Fig. 1, together with

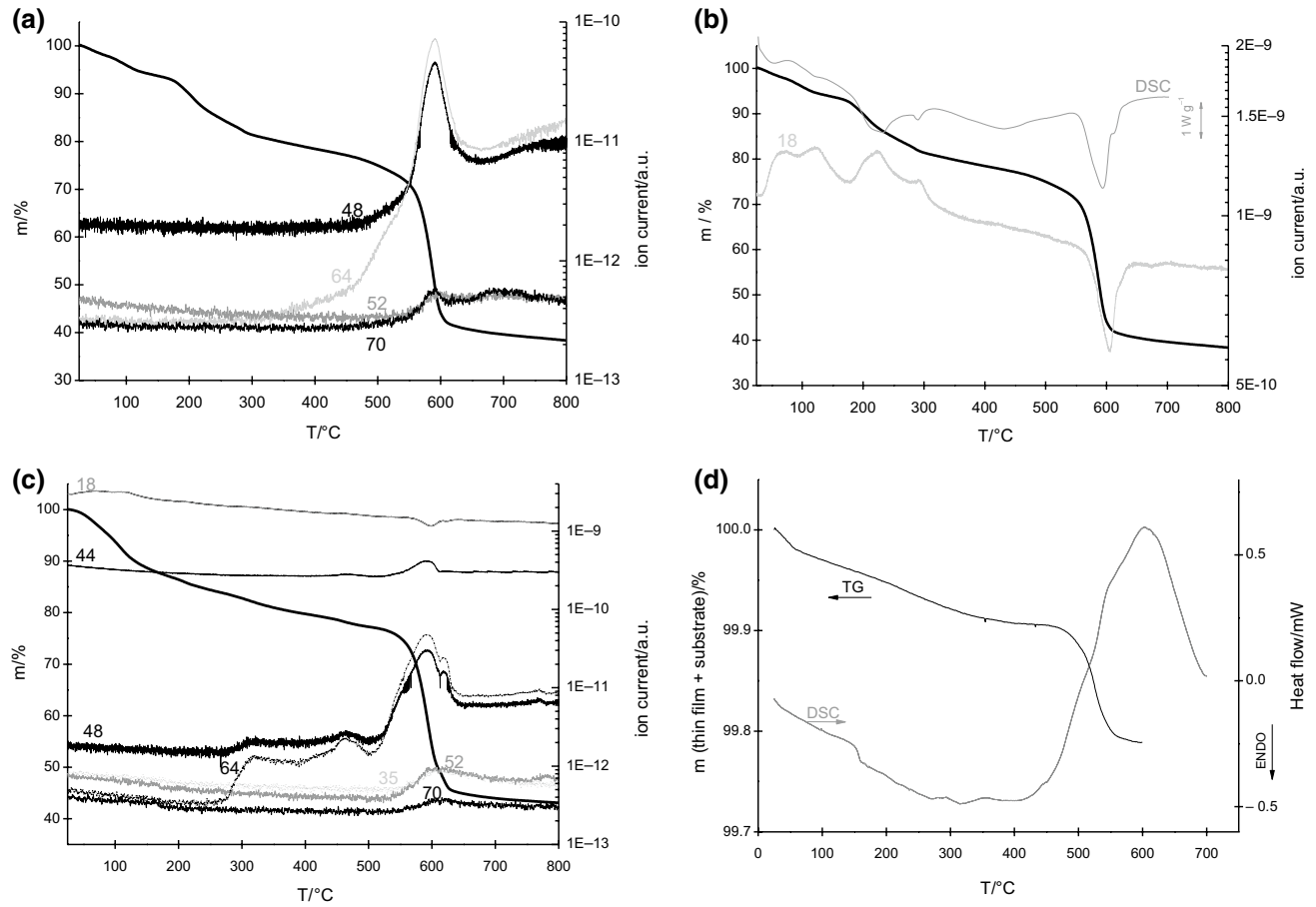

Fig. 1 **a** TG-MS curves of the xerogel, prepared without HPC addition; **b** TG and DSC curves of the same xerogel, together with MS signal for water; **c** TG-MS curves of the xerogel, prepared with HPC (0.3 mass%) and **d** TG and DSC curves of thin film (without HPC addition)

TG-DSC curves of the corresponding thin film (without addition of HPC). Thermal decomposition of the primary xerogel occurred in several successive steps (Fig. 1a). In the first one, from room temperature to 180 °C, dehydration occurred; evolution of water molecules is clearly seen from the $m/z = 18$ signal (Fig. 1b). In the next step, from 180 to 350 °C, water molecules are formed again; during this range, dehydroxylation process most probably took place. The rate of the mass loss is then slow to around 500 °C, but in this region (350–500 °C) a signal $m/z = 64$ indicates evolution of SO_2. In the last step, which is complete at 600 °C, chloride and sulfate counter ions, present in the xerogel due to preparation procedure, evolve in the form of SO ($m/z = 48$), SO_2 ($m/z = 64$), Cl_2 ($m/z = 70$) and HClO ($m/z = 52$), while water ($m/z = 18$) from the gaseous phase is consumed (Fig. 1b). Oxygen atoms from water maybe replace counter-ions, while hydrogen atoms could enable formation of hydroxyl groups on the surface of TiO_2 particles. All described steps are endothermic (Fig. 1b).

From the evolution of the diffractograms of intermediates (Fig. 2), it is obvious that crystallization of the anatase

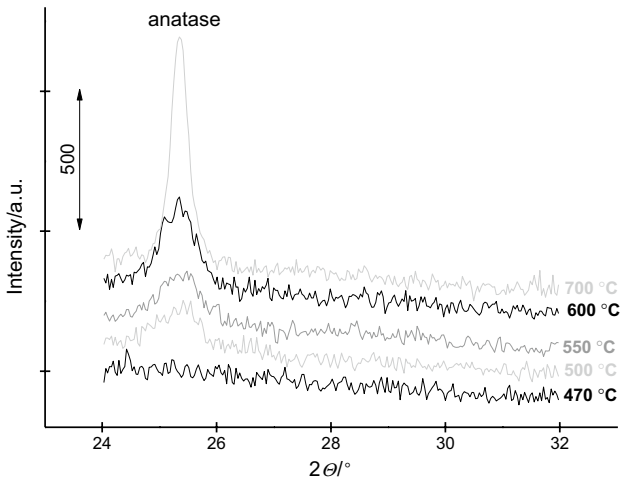

Fig. 2 X-ray diffractograms of thin films, deposited on a silicon substrate and thermally treated at selected temperature for 30 min

phase was possible after all of the counter ions were evolved. Thermal decomposition of a xerogel, prepared with addition of 0.3 mass% of HPC (Fig. 1c), is similar to decomposition of a primary one (Fig. 1a). Evolution of SO and SO_2 begins at approximately 50 degrees lower temperature, and therefore, this process is more overlapped with dehydroxylation; besides, their formation took place in three successive steps. During evolution of counter ions in the last step from 520 to 620 °C, a signal for CO_2 reflects thermal decomposition of polymeric HCP. TG and DSC curves of thin-film sample, deposited on a substrate, are presented in Fig. 1d). The reason for very small mass losses on a TG curve is small sample mass of the film, deposited on an inert substrate. In a thin-film sample, thermal decomposition of counter ions occurs at a lower temperature (onset temperature 490 °C) with regard to corresponding xerogel (onset temperature 550 °C) due to higher surface energy of nano-particles, while the lower endset temperature originates from smaller sample size. Similar behavior was already observed for nickel-oxide thin films [26]. A DSC curve of a thin film, deposited on a Pt substrate, shows intense exothermic peak due to anatase crystallization during evolution of counter ions.

XRD analysis of thin films

On the basis of DSC curve of thin film showing that crystallization of TiO_2 probably begins at around 470 °C, following temperatures of thermal treatment were selected: 470 °C, 500 °C, 550 °C, 600 °C and 700 °C. Films were treated at these temperatures for 30 min. The influence of duration of heat treatment (15 min, 30 min, 45 min and 60 min) on the anatase size grains was examined at 700 °C. Figure 2 shows X-ray diffraction patterns of thin films, thermally treated to a different degree, while in Table 1 the average anatase crystallite size is given.

From Fig. 2, it is evident that exposure to 470 °C or lower temperature is not sufficient to enable anatase crystallization. Most probably the lowest temperature needed is 500 °C since small grains (11 nm) are formed after 30 min. The size of the crystallites increases with the increase in processing temperature and reached nearly 30 nm after thermal treatment at 700 °C (Table 1). Phase change from anatase to rutile crystal modification occurred with increasing duration of thermal treatment at 700 °C. From Table 1, it is also evident that the rutile particles are two to three times larger from the anatase particles.

0.3 mass% of organic polymer HPC was added to sol to observe its effect on the photocatalytic activity of thin films and powders. Thermal treatment for 30 min at 550 °C, 600 °C and 700 °C was chosen. Results of XRD analysis does not indicate significant differences in particle size of thin films, treated at 550 °C and 600 °C, while anatase particles grew larger after 30 min thermal treatment at 700 °C; and rutile crystal modification is already present (Table 1).

Field emission scanning electron microscopy (FE-SEM)

Figure 3 represents plan and cross-sectional view of the film without (a, c) and with addition of HPC (b, d). It is evident that unmodified film does not contain pores; its surface is smooth, while the addition of HPC creates micrometer pores which are evenly distributed on the thin-film surface. After application of pollutant, its molecules can enter into pores and the surface for the photocatalytic reaction increased. Cross-sectional view shows that the thickness of the films, prepared from the unmodified sol, was around 100 nm while the addition of HPC enables formation of slightly thicker films (estimated thickness is around 130 nm).

Photocatalytic activity of thin films

FT-IR spectrum of thermally treated thin film (30 min at 700 °C), deposited on silicon substrate, is presented in Fig. 4a—black curve). Peak at 1070 cm^{-1} corresponds to Si–O–Si asymmetric stretching vibration [27], we ascribe its presence to oxide layer, formed on the top of the silicon resin. Peak positioned at 455 cm^{-1} corresponds to stretching

Table 1 Average particle size of anatase, obtained with XRD analysis

Temperature of thermal treatment/°C	Duration of thermal treatment/min	Anatase particle size/nm	Anatase particle size (addition of 0.3 mass% HPC) /nm
470	30	Amorphous	–
500	30	11	–
550	30	12	12
600	30	15	16
700	15	24	–
700	30	28	33; rutile present (110 nm)
700	45	30; rutile present (80 nm)	–
700	60	35; rutile present (90 nm)	–

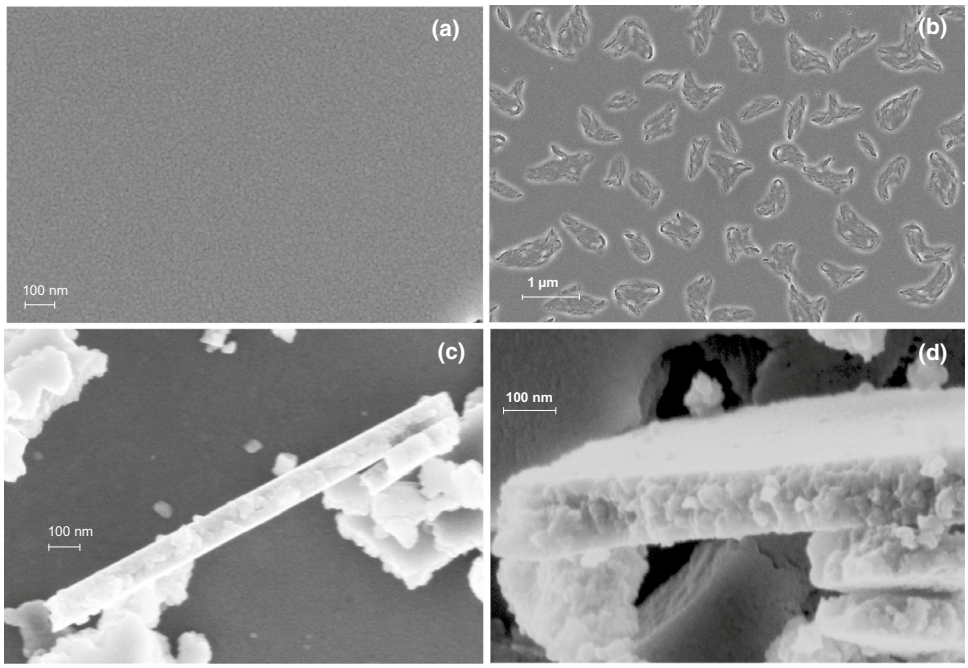

Fig. 3 FE-SEM images of thin films, thermally treated for 30 min at 700 °C: **a** planar view of the film, prepared from unmodified sol; **b** planar view of thin film, prepared with addition of 0.3 mass% HPC; **c** cross-sectional view for the unmodified films and **d** cross-sectional view for the films, prepared with addition of HPC

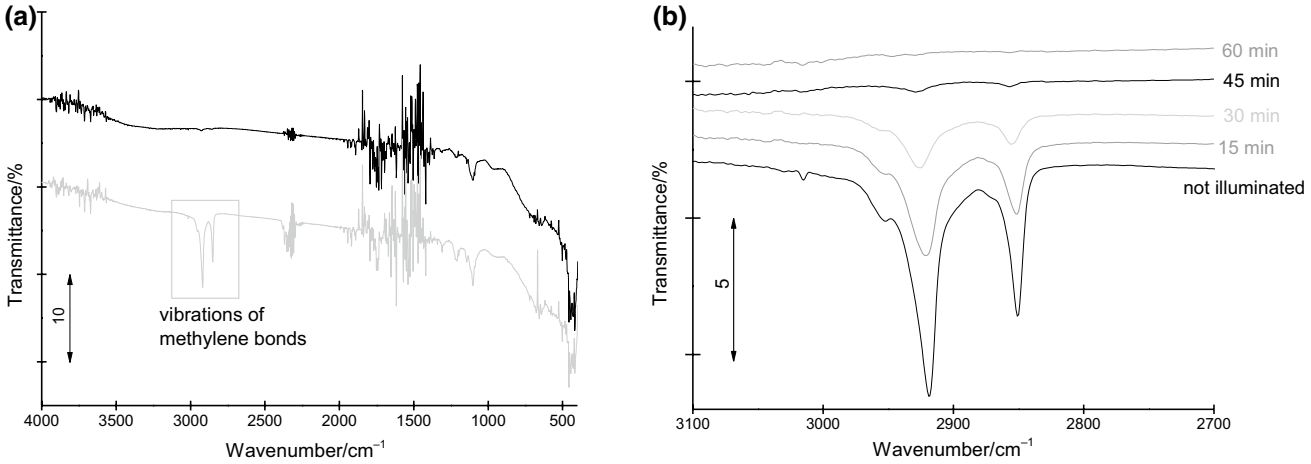

Fig. 4 **a** A comparison of FTIR spectra of bare thermally treated titania thin film (black curve) and after MS deposition (grey curve); **b** diminishing of the bands, originating from the asymmetric and symmetric stretching C-H vibrations in the region from 3100 cm^{-1} to 2700 cm^{-1} due to photocatalytic degradation of MS during UV-irradiation

vibration of Ti–O bond. After dip-coating of a methyl-stearate solution on the titania thin film and evaporation of the solvent, FTIR spectrum was recorded again. A significant absorption in the region from 3100 to 2700 cm^{-1} happened due to asymmetric (2920 cm^{-1}) and symmetric (2850 cm^{-1}) methylene stretching modes.

Photocatalytic activity was determined ex-situ on the basis of decreasing the intensity of the most intense peak, positioned at 2920 cm^{-1}. Thin films with deposited MS were placed into UV irradiation chamber for selected timeframes and after each irradiation period FT-IR spectra of thin films were recorded. During irradiation, MS degraded and degradation degree (α) was calculated on the basis of the following formula:

$$\alpha = 1 - \frac{h_t}{h_0}, \tag{1}$$

where h_t is the peak intensity after irradiation at a certain time and h_0 is the peak intensity prior to irradiation. Figure 4b shows evolution of the spectra with increasing irradiation time.

With the increasing temperature of thermal treatment, the degradation rate of MS on TiO_2 surface increases (Fig. 5a). Degradation process of MS on silicon substrate

and on thermally untreated titania film also occurs to a certain extent only due to illumination with UV light, but the degradation rate is low; degradation degree is lower than 10% after 90 min of illumination. Photocatalytic activity is enhanced after thermal treatment at 470 °C for 30 min. In this case, thin film is still amorphous; its photocatalytic activity is therefore low (after 90 min α reaches 31%). After crystallization of anatase phase (Table 1), photocatalytic activity became pronounced. In all cases, MS nearly completely degraded after being exposed for 60 min to UV light. The rate of MS degradation increased with increasing temperature of thermal treatment. Anatase grains grew larger in the case of higher temperature of thermal treatment (500 °C—11 nm, 550 °C—12 nm, 600 °C—15 nm and 700 °C—28 nm). Specific surface area decreases; therefore, lower photocatalytic efficiency was expected after thermal treatment at 600 °C and 700 °C. But on the other hand, lower degree of recombination due to the lower number of electron traps and decreasing of the band-gap in the samples with higher crystallinity result in the opposite effect [28], which seems to be predominant in our case.

Results of photocatalytic activity of titania thin films treated at 700 °C (Fig. 5b) from 15 to 60 min show that photocatalytic activity of thin films is influenced by various different factors. In general, activity of these films is similar, but there is no logical sequence in detailed course of the measured curves. It seems that the most efficient film was obtained with thermal treatment for 15 min in which anatase particles reached 24 nm. Thin film, treated for 30 min, exhibits the lowest efficiency (the size of anatase particles is 28 nm) after 15 min of illumination, but after that degradation rate increased and reached the value of the previously described film. Both films totally degraded MS after 45 min of illumination. Films which were exposed to 700 °C for 45 min or 60 min already contain rutile phase (Table 1), but their activity is comparable to the films previously described, which contain only anatase phase. Partial crystalline transformation of TiO_2 from anatase to rutile has lower effect than expected.

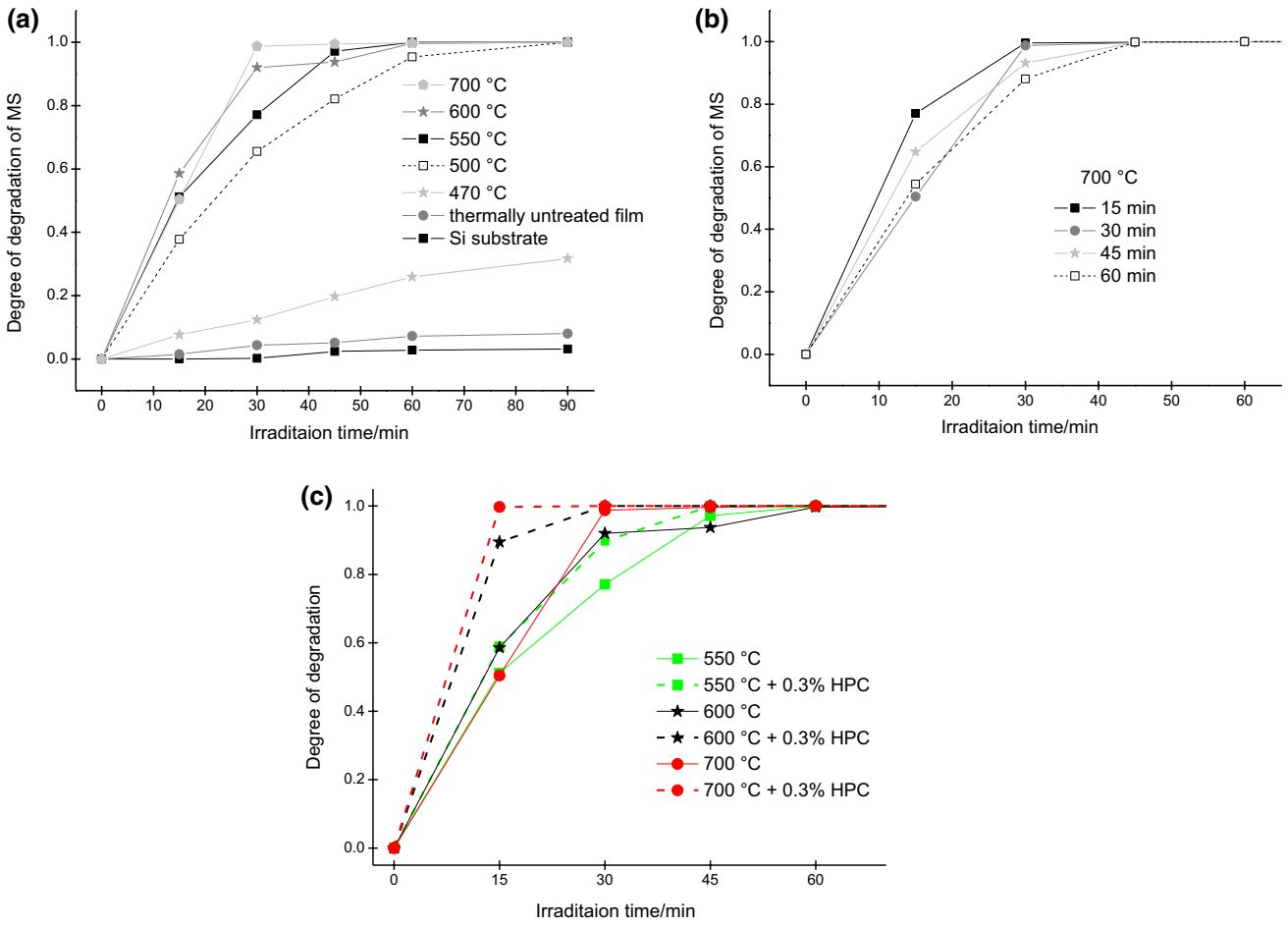

Fig. 5 The influence of **a** temperature of thermal treatment, **b** duration of thermal treatment at 700 °C and **c** the HPC addition; on the photocatalytic efficiency of titania thin films, thermally treated at selected temperatures for 30 min

On the basis of these results, we conclude that most probably, besides particle size and the presence of different crystalline modifications, additional factors, for instance thickness of thin film, also affect the photocatalytic activity. Figure 5c) shows a comparison in the rate of MS degradation with titania thin films, prepared from the primary sol and from the primary sol with addition of 0.3 mass% of HPC. Results of XRD analysis show that there is no significant difference in the size of anatase grains after thermal treatment at 550 °C or 600 °C (Table 1). But in both cases, the rate of MS degradation is faster in the case of HPC addition, most probably due to higher thickness of thin film and the presence of the pores (see Fig. 3). The highest rate of MS degradation was obtained with the films, thermally treated at 700 °C and with addition of HPC. In this case, the size of the anatase grains was larger (35 nm) compared with the film without addition of HPC (28 nm), and rutile was also present (Table 1). MS was degraded after 15 min of irradiation.

XRD and EDX analysis of xerogels

From the course of thermal decomposition of the xerogel (Fig. 1 a, b), we expected that anatase formation will occur after heating the sample to 600 °C or higher. Figure 6 presents diffractograms of the xerogel samples, thermally treated to the chosen temperature and left at the final temperature for 30 min. Evolution of SO_2 during thermal treatment leads to formation of $TiOSO_4$ phase (PDF 49–0467), which is observed as intermediate phase after thermal treatment at 400 °C, 500 °C and 600 °C. During the last step of decomposition between 520 °C and 620 °C anatase, crystalline modification is formed. The size of the grains is given in Table 2. In the case of thin film, anatase is formed already at 500 °C, whereas in the xerogel sample 100 degrees higher temperature is needed for its formation.

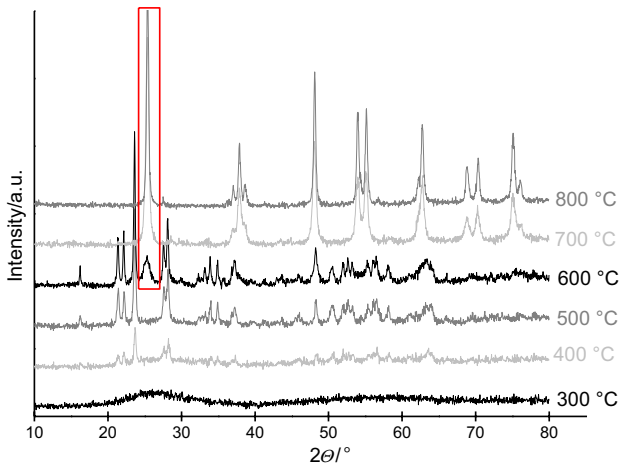

Fig. 6 Diffractograms of xerogel samples, thermally treated at selected temperature for 30 min. The most intense reflection of anatase phase, positioned at 25.4°, is put into frame

The presence of sulfur and chlorine content in thermally treated xerogel samples, used for photocatallytical efficiency tests, was determined using EDX spectrometry. Results are given in Table 3, showing that some sulfur remains in the thermally treated samples; its content decreases with increasing temperature of thermal treatment, whereas there is no chorine any more in the prepared samples. It was already confirmed with XPS measurements that sulfur was intersticially doped into TiO_2 matrix [29].

Photocatalytic activity of powdered samples

Photocatalytic activity of xerogels without and with addition of 0.3 mass% of HPC and thermally treated at 630 °C, 700 °C and 750 °C for 30 min was studied. After the thermal treatment, all obtained powders were white, indicating that all organic additives decomposed. Particle sizes, obtained with different thermal treatment protocols, are presented in Table 4 together with the size of the anatase particles, specific surface area and photocatalytic activity. From the comparison of Fig. 6 and Table 4, it is evident that after 30 min of thermal treatment at 630 °C $TiOSO_4$ phase disappeared and β-TiO_2 (PDF 46–1237) is formed.

Table 2 Presence of crystalline phases and average particle size of anatase in intermediate samples of xerogels, thermally treated at different final temperature

Temperature of thermal treatment/°C	Anatase particle size/nm
300	–
400	–
500	–
600	5
700	19
800	32

Table 3 Sulfur contents in xerogel samples, thermally treated for 30 min at 630 °C, 700 °C and 750 °C

Sample	Temperature of thermal treatment/°C	mass percentages of S
Primary xerogel	630	0.97
	700	0.32
	750	0.27
Primary xerogel + 0.3 mass% HPC	630	1.04
	700	0.42
	750	0.19

Degradation rate of iso-propanol is increasing with the increasing temperature of thermal treatment. Lowest photocatalytic activity possesses sample, thermally treated at the lowest temperature, 630 °C and with addition of HPC. The size of the anatase particles is 17 nm, and the sample still contains some β-TiO_2. Specific surface area (SSA) is around 105 $m^2\ g^{-1}$ and is very similar to SSA of xerogel without addition of HPC. However, activity of this sample is higher, probably due to larger anatase grains (20 nm—Table 4). With the increase in processing temperature to 700 °C, the content of anatase, present in the sample, increases. Particle size also increased (33 nm), which results in smaller active surface, around 70 $m^2\ g^{-1}$. The rate of iso-propanol degradation is higher in the case of smaller anatase particles (29 nm), which were obtained in the xergoel with the addition of HPC. Photocatalytic activity of both powders, thermally treated at the highest temperature, 750 °C, increased. In this case, the diameter of anatase particles is more than 40 nm, whereas SSA decreased to around 50 $m^2\ g^{-1}$. The highest activity was obtained by sample with addition of HPC and almost reached the one from commercially available P25. The results show that for good activity better crystallinity is more important parameter than specific surface area.

Discussion

Thermal analysis, in connection with X-ray diffraction, proved to be powerful technique which enables to follow crystallization of titania from amorphous phase, prepared by sol–gel synthesis. When counter ions (in the case of our study sulfate ones) started to evolve, detected as a mass loss on TG curve and the observed decomposition is confirmed with TG-MS coupled technique with evolution of SO_2 and SO, crystallization process starts. Evolved gasses are more easily detected in the case of xerogel samples, since the signal in mass spectrometer is higher due to sufficient quantity of the evolved gas. Onset and endset decomposition temperatures usually differ when thermal decomposition of xerogel is compared with thermal decomposition of thin films (under identical measurement conditions, i.e., heating rate, atmosphere, rate of the purge gas) for several reasons: (1) Thin films with a thickness of some tenth of nanometers can be composed of nanoparticles with large number of surface atoms, having high surface energy and are therefore more reactive; thermal decomposition occurs at lower temperatures. (2) Influence of substrate on the behavior and consequently thermal stability of thin film with regard to xerogel samples. (3) Low thickness of thin films, enabling fast diffusion of the evolved gases on the surface of solid phase.

In this study, evolution of sulfate anions begins at 490 °C (onset T) in the case of thin-film sample, supported on a substrate, while for xerogel sample this temperature was at 550 °C. XRD analysis and measurements of photocatalytic activity show that film, treated for 30 min at 470 °C, is still amorphous. Exposure to 500 °C for 30 min enables formation of the anatase phase with the size of the particles of 11 nm. At higher temperatures of thermal treatment (550 °C, 600 °C and 700 °C), larger anatase particles were obtained; the rate of pollutant degradation increased with increasing size of the particles. Films, exposed to 700 °C for more than 30 min, contain both, anatase and rutile modification; but the photocatalytic activity was nearly independent on the presence of both phases. Time needed to completely degrade model pollutant methyl stearate under UV illumination, was 90 min and 30 min using thin films, treated at 500 °C and 700 °C, respectively. Although the size of the anatase nanoparticles reached 28 nm in the latter case, and the specific surface area decreased, better crystallinity in more thermally

Table 4 Temperature of thermal treatment, anatase particle sizes, specific surface area and photocatalytic activity of powders, obtained after 30 min of thermal treatment of selected xerogels

Sample	Temperature of thermal treatment/°C	Anatase particle size/nm	Specific surface area/ $m^2\ g^{-1}$	Comment	Photocatalytic activity/ppm h^{-1}
Primary xerogel	630	20	104	β-TiO_2 still present in small amount	740
	700	33	69	β-TiO_2 still present, slightly observable	770
	750	45	53		960
Primary xerogel + 0.3 mass% HPC	630	17	104	β-TiO_2 still present in small amount	660
	700	29	73	β-TiO_2 still present, slightly observable	1080
	750	41	51		1220
P25			Commercially available sample		1320

treated films had predominant effect on the photocatalytic efficiency.

In xerogel samples, formation of anatase phase begins at higher temperatures with regard to thin films, i.e., at 600 °C. Therefore, prepared xerogels were thermally treated at 630 °C, 700 °C and 750 °C for 30 min. Their photocatalytic activity was observed by monitoring the rate of isopropanol conversion into acetone. In most cases, the increase in the processing temperature resulted in the increase in the photocatalytic activity. Powders, which were obtained from the unmodified sol and processed at 630 °C and 700 °C contained also β-TiO_2, which most likely is not very efficient photocatalyst since photocatalytic activity of powders not containing β-TiO_2 was higher. Anatase particle size increased with the increasing temperature of thermal treatment and ranged from 20 to 45 nm.

Conclusions

Photocatalytically active thin films and powders were prepared by the sol–gel route using $TiCl_4$ as a precursor. Thin films were deposited on a substrate by dip coating technique. After silicon resins were coated with the prepared sol, the system was left to dry and afterwards thermally treated. To enhance photocatalytic activity, organic polymer hydroxypropyl cellulose was added to the primary sol. Powders were obtained by drying the sol, followed by thermal treatment.

Sol preparation procedure was simple since neither cooling nor centrifugation was required. Most complicated step of the synthesis was dissolving $TiCl_4$ in the acidified water. Stability of the prepared sols was good. The biggest drawback of the prepared sols is that they are suitable only for use on acid-resistant surfaces (ceramics, glass, enamel).

With the help of coupled TG-MS measurement of xerogels and thin films, deposited on a substrate, onset temperature of anatase formation from amorphous phase was determined, confirmed with x-ray diffraction. At higher temperatures crystallization occurs, and with increased time of duration of thermal treatment, anatase grains grow or can transform to thermodynamically stable rutile. Since several factors (specific surface area, band gap and crystalline phase present) influence the photocatalytic efficiency of titania, optimal thermal treatment should be determined.

For thin films, photocatalytic efficiency was tested as the rate of model fatty compound methyl stearate decomposition under UV illumination using ex-situ FTIR spectroscopy. The highest rate of MS degradation was obtained with the films, thermally treated at 700 °C and with addition of 0.3 mass% of HPC (MS degraded in 15 min of illumination). Very high efficiency of these films, which contained anatase particles with a diameter of 35 nm, and nearly three times larger rutile particles, was ascribed to their porous structure and larger thickness.

Photocatalytic efficiency of xerogels was tested as the rate of isopropanol degradation under UV illumination using in-situ FT-IR spectroscopy. Most photocatalytically active was powder, prepared from sol with addition of 0.3 mass% HPC and thermally treated at 750 °C, which almost reached activity of commercially available P25.

Results show that optimization of photocatalytic activity is not usually straightforward and depends on a broad range of different factors. Addition of HPC is promising for optimizing photocatalytic activity of TiO_2.

Acknowledgements The authors acknowledge the financial support provided by the Slovenian Research Agency (research core funding Nos. P1-0134 and P2-0273). The authors are grateful to Dr. Nejc Rozman for BET measurements.

References

1. Lee JD. Concise inorganic chemistry. 4th ed. New York: Chapman & Hall; 1991. p. 684–696.
2. Chen X, Selloni A. Introduction: titanium dioxide (TiO_2) nanomaterials. Chem Rev. 2014. https://doi.org/10.1021/cr500422r.
3. Carp O, Huisman CL, Reller A. Photoinduced reactivity of titanium dioxide. Prog Solid State Ch. 2004. https://doi.org/10.1016/j.progsolidstchem.2004.08.001.
4. Addamo M, Bellardita M, Di Paola A, Palmisano L. Preparation and photoactivity of nanostructured anatase, rutile and brookite TiO_2 thin films. Chem Commun (Camb). 2006. https://doi.org/10.1039/B612172A.
5. Saadati F, Keramati N, Ghazi MM. Influence of parameters on the photocatalytic degradation of tetracycline in wastewater: a review. Crit Rev Environ Sci Tec. 2016. https://doi.org/10.1080/10643389.2016.1159093.
6. Hočevar M, Opara Krašovec U, Bokalič M, Topič M, Veruman W, Brandt H, Hinsch A. Sol-gel based TiO2 paste applied in screen-printed dye-sensitized solar cells and modules. J Ind Eng Chem. 2013. https://doi.org/10.1016/j.jiec.2012.12.046.
7. Fröschl T, Hörmann U, Kubiak P, Kučerová G, Pfanzelt M, Weiss CK, Behm RJ, Hüsing N, Kaiser U, Landfester K. Wohlfahrt-Mehrens M High surface area crystalline titanium dioxise: potential and limits in electochemical energy storage and catalysis. Chem Soc Rev. 2012. https://doi.org/10.1039/C2CS35013K.
8. Kamat PV. A Conversation with Akira Fujishima. ACS Energy Lett. 2017. https://doi.org/10.1021/acsenergylett.7b00483.
9. Hashimoto K, Irie H, Fujishima A. TiO_2 photocatalysis: a historical overview and future prospects. Jpn J Appl Phys. 2005. https://doi.org/10.1143/JJAP.44.8269.
10. Topalov AS, Šojić DV, Molnar-Gabor DA, Abramović BF, Čomor MI. Photocatalytic activity of synthesized nanosized TiO2 towards the degradation of herbicide mecoprop. Appl Catal B-Environ. 2004. https://doi.org/10.1016/j.apcatb.2004.06.012.
11. Lavrenčič Štangar U, Černigoj U, Maver K, Trebše P, Gross S. TiO2-anatase films made by sol-gel processing and their photodegradation activity towards pollutants in water. In: Benjamin MG, editor. New research on thin solid films. New York: Nova Science Publishers; 2007. p. 107–132.
12. Sasirekha N, Rajesh B, Chen Y-W. Synthesis of TiO_2 sol in a neutral solution using TiCl4 as a precursor and H2O2 as an

oxidizing agent. Thin Solid Films. 2009. https://doi.org/10.1016/j.tsf.2009.06.015.
13. Krýsa J, Keppert M, Jirkovský J, Štengl V, Šubrt J. The effect of thermal treatment on the properties of TiO_2 photocatalyst. Mater Chem Phys. 2002. https://doi.org/10.1016/j.matchemphys.2004.03.021.
14. Meroni D, Pifferi V, Sironi B, Cappelletti G, Falciola L, Ardizzone S. Block copolymers for the synthesis of pure and Bi-promoted nano-TiO_2 as active photocatalysts. J Nanopart Res. 2012. https://doi.org/10.1007/s11051-012-1086-z.
15. Hao WC, Zheng SK, Wang C, Wang TM. Comparison of the photocatalytic activity of TiO2 powder with different particle size. J Mater Sci Lett. 2002. https://doi.org/10.1023/A:1020386019893.
16. Zhigo Z, Wang CC, Zakaria R, Ying JY. Role of particle size in nanocrystalline TiO_2-based photocatalysts. J Phys Chem B. 1998. https://doi.org/10.1021/jp982948+.
17. Hossoingholi M, Pazouki M, Hosseinnia A, Aboutalebi SH. Room temperature synthesis of nanocrystalline anatase sols and preparation of uniform nanostructured TiO_2 thin films: optical and structural properties. J PhysD Appl Phys. 2011. https://doi.org/10.1088/0022-3727/44/5/055402.
18. Ohtani B, Ogawa Y, Nishimoto S. Photocatalytic activity of amorphous−anatase mixture of titanium(IV) oxide particles suspended in aqueous solutions. J Phys Chem B. 1997. https://doi.org/10.1021/jp962702+.
19. Porter JF, Lee Y-G, Chan CK. The effect of calcination on the microstructural characteristics and photoreactivity of Degussa P-25 TiO_2. J Mater Sci. 1999. https://doi.org/10.1023/A:1004560129347.
20. Shan AY, Ghazi TIM, Rashid SA. Immobilization of titanium dioxide onto supporting materials in heterogenous photocatalysis: a review. Appl Catal A-Gen. 2010. https://doi.org/10.1016/j.apcata.2010.08.053.
21. Pelaez M, Nolan NT, Pillai SC, Seery MK, Falaras P, Kontos AG, Dunlop PSM, Hamilton JWJ, Byrne JA, O'Shea K, Entezari MH, Dionysiou DD. A review on the visible light active titanium dioxide photocatalysts for environmental applications. Appl Catal B Environ. 2012. https://doi.org/10.1016/j.apcatb.2012.05.036.
22. Qu Y, Duan X. Challenge and perspective of heterogeneous photocatalysts. Chem Soc Rev. 2013. https://doi.org/10.1039/C2CS35355E.
23. Marolt T, Sever Škapin A, Bernard J, Živčec P, Gaberšček M. Photocatalytic activity of anatase-containing facade coatings. Surf Coat Tech. 2011. https://doi.org/10.1016/j.surfcoat.2011.08.053.
24. Tasbihi M, Lavrenčič Štangar U, Sever Škapin A, Ristić A, Kaučič V, Novak TN. Titania-containing mesoporous silica powders: structural properties and photocatalytic activity towards isopropanol degradation. J Photoch Photobio A. 2010. https://doi.org/10.1016/j.jphotochem.2010.07.011.
25. Rozman N, Tobaldi DM, Cvelbar U, Puliyalil H, Labrincha JA, Leagt A, Sever ŠA. Hydrothermal synthesis of rare-earth modified Titania: influence on phase composition, optical properties, and photocatalytic activity. Materials. 2019. https://doi.org/10.3390/ma12050713.
26. Cerc Korošec R, Bukovec P. Sol-gel prepared NiO thin films for electrochromic applications. Acta Chim Slov. 2006;53:136–47.
27. Gillespie RJ. ROBINSON EA, Characteristic vibrational frequencies of compounds containing Si-0-Si, P-0-P, S-0-S, and C1-0-C1 bridging groups. Can J Chem. 1964;42:2496–503.
28. Tanaka Y, Suganuma M. Effects of heat treatment on photocatalytic property of sol–gel derived polycrystalline TiO_2. J Sol-Gel Sci Techn. 2001. https://doi.org/10.1023/A:1011268421046.
29. Žener B, Matoh L, Carraro G, Miljević B, Cerc-Korošec R. Sulfur, nitrogen and platinum doped and co-doped titania thin films with high catalytic efficiency under visible light illumination. Beilstein J Nanotechnol. 2018. https://doi.org/10.3762/bjnano.9.155.